

Longitudinal Compressive Failure of Multiple-Fiber Model Composites for a Unidirectional Carbon Fiber Reinforced Plastic

Tae Kun Jeong, Masahito Ueda

Department of Mechanical Engineering, College of Science and Technology, Nihon University, Tokyo, Japan
Email: cste13001@g.nihon-u.ac.jp

Received 11 November 2015; accepted 5 January 2016; published 8 January 2016

Copyright © 2016 by authors and Scientific Research Publishing Inc.

This work is licensed under the Creative Commons Attribution International License (CC BY).

<http://creativecommons.org/licenses/by/4.0/>



Open Access

Abstract

The longitudinal compressive failure of a unidirectional carbon fiber reinforced plastic (CFRP) was studied using multiple-fiber model composites. Aligned carbon fibers were embedded in an epoxy matrix and put on a rectangular beam. A compression test of the model composite was performed by means of a four point bending test of the rectangular beam. The number of carbon fibers was changed from one to several thousands, by which the effect on compressive failure modes was investigated. A compressive failure of a single-fiber model composite was fiber crush. The fiber crush strain was much higher than the compressive failure strain of the unidirectional carbon fiber reinforced plastic. By contrast, a compressive failure of a multiple-fiber model composite was kink-band. The longitudinal compressive failure mechanism shifted from fiber crush to kink-band due to an increasing number of fibers. Kink-band parameters *i.e.* kink-band angle and kink-band width were dependent on the number of closely-aligned carbon fibers.

Keywords

Polymer Matrix Composite, Carbon Fiber, Compressive Failure, Kink-Band, Model Composite

1. Introduction

Unidirectional carbon fiber reinforced plastic (CFRP) is used as a structural material for aircraft because of its superior specific stiffness, strength and fatigue resistance as compared to other metallic materials typically used in aircraft fabrication. Unidirectional CFRP is composed of reinforcing continuous carbon fibers within a poly-

How to cite this paper: Jeong, T.K. and Ueda, M. (2016) Longitudinal Compressive Failure of Multiple-Fiber Model Composites for a Unidirectional Carbon Fiber Reinforced Plastic. *Open Journal of Composite Materials*, 6, 8-17.

<http://dx.doi.org/10.4236/ojcm.2016.61002>

mer matrix, which causes an unbalanced mechanical property between tension and compression. Compressive failure typically occurs at 50% - 60% of the tensile stress failure point [1]. Although the overall tensile strength of unidirectional CFRPs has been increasing because of research and development into reinforcing carbon fibers, the compressive strength remains almost constant. The upper limit of the compressive strength is approximately 1800 MPa [2]. If a unidirectional CFRP is used as a beam structure, thereby carrying a bending moment, the compression side may fail prior to the tension side. This failure mechanism indicates that compressive strength is a critical design issue for CFRP structures. An increased understanding of the compressive failure mechanisms will lead to improved reliability of structures using unidirectional CFRP.

Kink-band failure is a typical mode of longitudinal compressive failure for a unidirectional CFRP. It results from an in-phase, micro-buckling of the fibers within the polymer matrix. The kink-band failure occurs instantaneously resulting in a sudden loss of the load. Kink-band failure is known as a primary cause of low compressive strength. Many experimental research efforts into kink-band failure have been published [3]-[17]. Kink-band parameters, *i.e.* kink-band angle and kink-band width, are summarized in **Table 1**. The kink-band parameters are dependent on the material system and fiber volume fraction, which can affect resultant compressive strength.

A model composite is used to study the fundamental fracture mechanism of a CFRP [18]-[24]. A compression test of a single-fiber model composite showed that the compressive failure was due to fiber crush when the epoxy matrix was sufficiently stiff to prevent buckling of the embedded carbon fiber [23]. The compressive strength of a carbon fiber is higher than that of the unidirectional CFRP, thereby indicating a nonlinear stress-strain relation when in compression [2] [21]. The different fracture modes between a single-fiber model composite and a unidirectional CFRP indicate that the number of carbon fibers affects the fracture modes and resultant compressive strength.

For this research, compression tests of multiple-fiber model composites were performed to study kink-band failure mechanisms. A compression test of a single-fiber model composite was performed to measure the compressive failure strain due to fiber crush. Since the fracture mode depends on the number of closely aligned carbon fibers, the mutually interacting distance between each fiber is studied using a two-fiber model composite. Then multiple-fiber model composites were made in which distance between the fibers was less than the mutually interacting distance. The number of carbon fibers in the multiple-fiber model composites was then increased which resulted in the compressive failure mode shifting from fiber crush failure to kink-band failure. The kink-band failure parameters were dependent on the number of closely aligned carbon fibers.

2. Experiment Arrangement

2.1. Materials

Model composites were made of carbon fibers and epoxy resin. A polyacrylonitrile based carbon fiber (T800 S-24 K-10 E, Toray Industries) was used with the mechanical properties shown in **Table 2** [25]. A carbon fiber was taken from a 24,000 tow supplied by the manufacturer. An epoxy resin (105/206, West system) was selected that cured at room temperature.

Table 1. Kink-band parameters and compressive strength.

Fiber/Matrix	Fiber volume fraction V_f [%]	Kink-band angle β [degree]	Kink-band width ω [μm]	Compressive strength σ_c [MPa]
T800/924C [3] [7]	65	5 ~ 30	60 ~ 80	1485
AS4/PEEK (APC-2) [4]	60	12 ~ 16.5	76 ~ 255	1210
IM7/PEEK (APC-2) [5]	60	10 ~ 35	270	-
AS4/PEEK [8]	60	14	175	-
IM7/8552 [11]	-	~23	-	1570
T800/924C [11]	-	5 ~ 30	90	1625
HTS40/977 - 2 [14]	58	10 ~ 25	60 ~ 100	1396
T800/924 [15]	63	~20	150	1296
T800S/2592 [17]	65	25	100	1450

Table 2. Properties of T800 S carbon fiber [25].

Tensile modulus	Tensile strength	Tensile failure strain	Diameter
294 GPa	5880 MPa	2.0%	5 μm

A unidirectional CFRP laminate was also fabricated using a unidirectional prepreg tape (T800SC/#2592, Toray Industries). The fiber volume fraction of the laminate was approximately 65%. The compression test was performed in accordance with ASTM D695 using an end-loading test fixture [26]. Average applied compressive strain and compressive strength were $0.92\% \pm 0.025\%$ and $1445 \text{ MPa} \pm 55.9 \text{ MPa}$, respectively.

2.2. Configuration of the Model Composites

2.2.1. Single-Fiber Model Composite

A single-fiber model composite was prepared to study the longitudinal compressive failure of the carbon fiber. The specimen configuration is shown in **Figure 1**. As a base for the compression test, a beam was made from epoxy resin. The epoxy beam was a square cross-section of 10 mm in height and width, and 150 mm in length. Four copper films were wrapped at intervals of 110 mm and 134 mm respectively. The copper film was 2 mm in width and 0.01 mm in thickness. A single carbon fiber was attached to the surface of an epoxy beam with one end of the carbon fiber adhered to the epoxy beam using cyanoacrylate adhesive. An aluminum weight was adhered to the other end of the carbon fiber to straighten the fiber. A prestress of 500 MPa was applied to the carbon fiber. Then, the carbon fiber and copper films were soldered. The carbon fiber were finally molded with epoxy and fully coated and adhered to the epoxy beam. The molded thickness was approximately 0.7 mm or less after being shaved using sandpaper. The surface of the beam was then polished using an abrasive compound to allow for observation of the carbon fiber. The epoxy resin was cured at room temperature to prevent thermal residual stress from developing in the molding. In order to prevent debonding of the epoxy resin from the epoxy beam during a four-point bending test, a scratch was made on the epoxy beam by a standard box cutter. A strain gauge (KFG-2 - 120, Kyowa) was glued onto the same side of the beam as the carbon fiber and molded together with carbon fibers to measure compressive strain during the compression test.

2.2.2. Two-Fiber Model Composite

A two-fiber model composite was prepared to study the effect of adjacent carbon fiber distances during compression failure. Two carbon fibers were temporarily adhered to small and large C-shaped aluminum jigs using cyanoacrylate adhesive as shown in **Figure 2(a)**. Then the C-shaped jigs were set on a XYZ platform. The platform was controlled to closely align the two carbon fibers. The two carbon fibers were again temporarily adhered to the small C-shaped jig as shown in **Figure 2(b)**. The fibers were then cut and the large C-shaped jig was removed. The two carbon fibers attached to the small C-shaped jig were installed on the epoxy beam (10 mm in height and width and 140 mm in length). Finally, the carbon fibers were molded with the epoxy resin. The molded thickness was shaved and polished using the same process as described in Section 2.2.1. The specimen configuration is shown in **Figure 3**. Five two-fiber model composites were prepared by changing distances between the two carbon fibers as follows: 0 μm , 2 μm , 7 μm , 9 μm , and 15 μm .

2.2.3. Multiple-Fiber Model Composite

A multiple-fiber model composite was prepared to study the effect of the number of carbon fibers on the kink-band failure. The specimen configuration is shown in **Figure 4**. Closely aligned multiple carbon fibers were attached to the epoxy beam and then molded with epoxy resin. The molded thickness was shaved and polished using the same process as described in Section 2.1.1. The number of fibers was changed as follows: 3, 4, 8, 10, 530, 8000, and 11,000. The fibers were taken one by one from a 24,000 tow when the test quantity of carbon fiber was less than 10. The fibers were counted by weight after being taken from a 24,000 tow when the test quantity was larger than 10 fibers. The distance between each fiber was not controlled but was smaller than 15 μm based on the result in Section 3.2. This was confirmed by observing the specimen cross-section using a digital microscope with a charge-coupled device (CCD) camera (MSZ-125, Asahikogakuki).

2.3. Compression Test of Model Composite

The compression tests of the model composites were performed by means of a four-point bending test. The

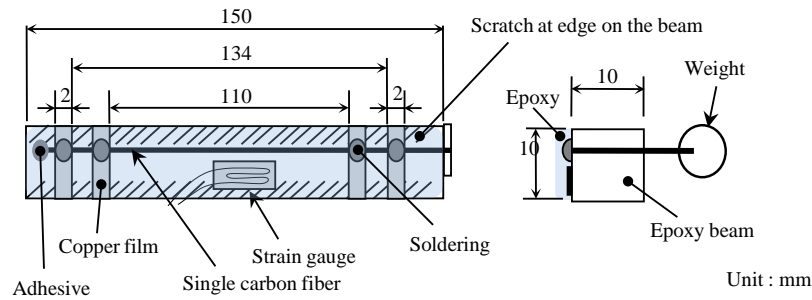


Figure 1. Specimen configuration of a single-fiber model composite.

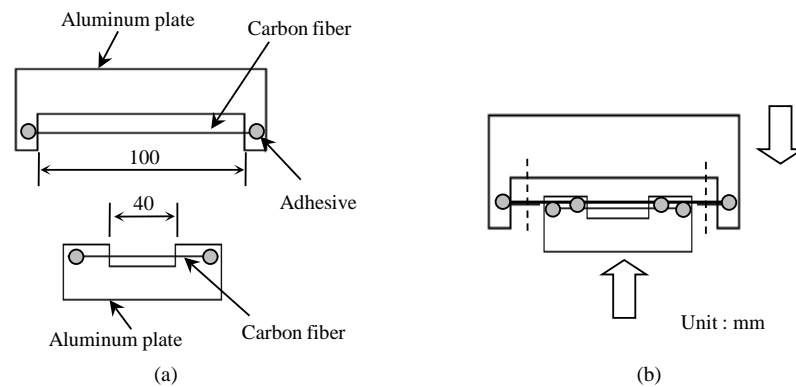


Figure 2. Procedure to closely align carbon fibers.

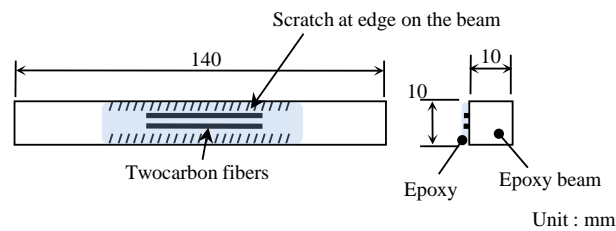


Figure 3. Specimen configuration of a two-fiber model composite.

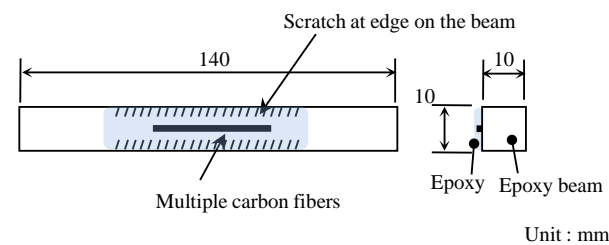


Figure 4. Specimen configuration of a multiple-fiber model composite.

schematic of the four-point bending test is shown in **Figure 5**. Since the carbon fibers were embedded in an epoxy matrix on the epoxy beam, the four-point bending test of the epoxy beam was performed so as to develop a compressive strain in the carbon fibers. A loading span of 100 mm with a supporting span of 20 mm was used for the single-fiber model composite, as shown in **Figure 5(a)**. A loading span of 130 mm and with a supporting span of 30 mm was used for the other model composites, as shown in **Figure 5(b)**.

2.4. Measurement of Electrical Resistance of a Carbon Fiber during Compression Test

The electrical resistance of a carbon fiber was measured by means of a four-probe method during the compression

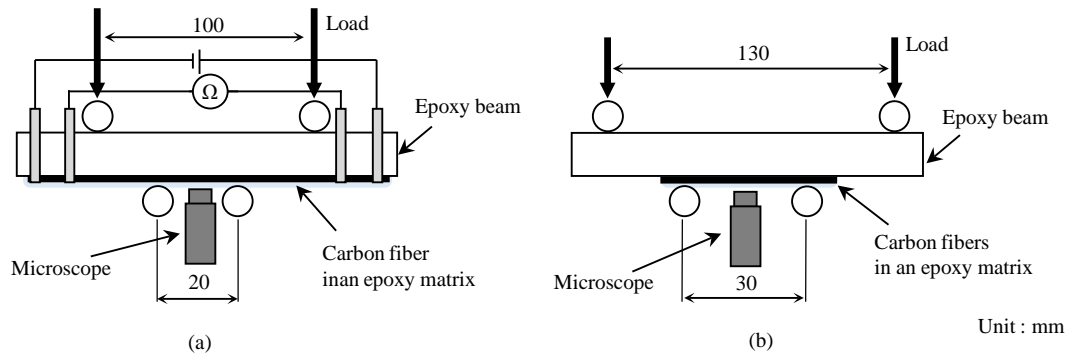


Figure 5. Schematic of a four-point bending test. (a) Single-fiber model composite; (b) Two-fiber and multiple-fiber model composite.

test to detect the onset of compressive failure. Electrical resistance of a carbon fiber R is expressed as:

$$R = \rho \frac{L}{A} \quad (1)$$

where ρ is specific electrical resistance, L is length, and A is cross-sectional area.

Electrical resistance of a carbon fiber decreases with an increase in compressive load due to the shortening of the fiber. If a carbon fiber fractures, electrical resistance increases. Electrical resistance of a carbon fiber was only measured in compression test of a single-fiber model composite to precisely detect the onset of fiber compressive failure and measure compressive failure strain. Electrical resistance of the carbon fiber was measured using a LCR HiTester, Model 3522 from Hioki.

3. Results and Discussion

3.1. Compressive Failure of a Single-Fiber Model Composite

The compression test of a single-fiber model composite was performed by means of a four-point bending test. **Figure 6** shows an example of the electrical resistance change ratio due to compressive loading. The ordinate shows the electrical resistance change ratio. The abscissa shows the compressive strain of the carbon fiber measured using the strain gauge. The electrical resistance of the carbon fiber decreased as the compressive strain increased. Electrical resistance then increased due to the onset of compressive failure. The compressive failure strain was approximately 2.5% which included the pre-strain of approximately 0.17%. This strain value was much higher than that of the unidirectional CFRP fabricated using a unidirectional prepreg tape (see Section 2.1). This indicates that the compressive failure mechanism of a unidirectional CFRP is different from that of a single-fiber model composite. The difference between the single-fiber model composite and a unidirectional CFRP is explained by the difference in the number of carbon fibers as discussed in the following sections.

Compressive failure of a carbon fiber once the compressive load was completely removed is shown in **Figure 7**. The compressive loading was maintained after the increase in electrical resistance was observed to ensure the fiber fracture fully developed. Once the fracture, or crush, was fully developed, the load was removed. The fiber fractured in shear at an angle β , which was approximately 40° . The angle was different from the kink-band angle for a unidirectional CFRP (see **Table 1**). Additionally, it has been reported that carbon fiber fails by buckling when the stiffness of the epoxy matrix is low [23]. However, the epoxy matrix was sufficiently stiff to prevent buckling of a carbon fiber.

3.2. Mutual Interaction of Carbon Fibers during Compressive Failure

The compression test of a two-fiber model composite was performed by means of a four point bending test. The compressive failure of the carbon fibers after the compression test is shown in **Figure 8**. The figure shows the fiber fracture after the compressive load was removed. The fracture point of the two carbon fibers was observed at almost same location. This would indicate mutual interaction between adjacent fibers during compressive failure when the distance between each fiber was less than $15 \mu\text{m}$. From this result, multiple-fiber model composites were made with a distance between each fibers of less than $15 \mu\text{m}$.

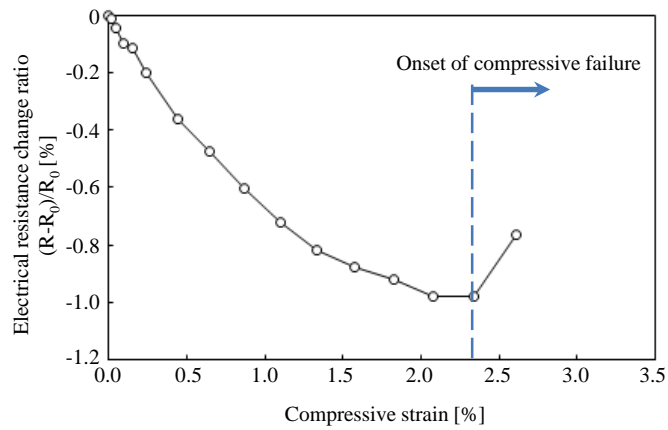


Figure 6. A typical example of electrical resistance change ratio of a carbon fiber due to compressive loading.

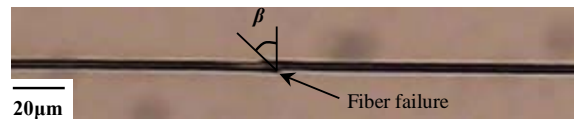


Figure 7. Compressive failure of a single-fiber model composite.

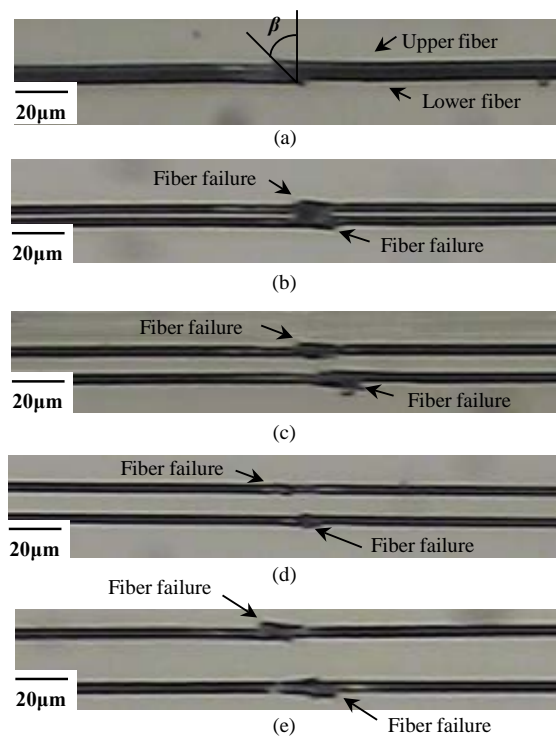


Figure 8. Compressive failure of two-fiber model composites. (a) 0 μm spacing between fibers; (b) 2 μm spacing between fibers; (c) 7 μm spacing between fibers; (d) 9 μm spacing between fibers; (e) 15 μm spacing between fibers.

3.3. Compressive Failure of a Multiple-Fiber Model Composite

The compression test of a multiple-fiber model composite was performed by means of a four-point bending test.

The distances between each fiber were less than 15 μm based on the results discussed in Section 3.2 where the fibers interacted mutually during compressive failure. The number of carbon fibers was increased from 3 to 11,000 to investigate the effect on the compressive failure. For the purposes of this research, the term “fiber volume fraction” is not used to describe model composites since the fraction is almost zero because the fiber embedded area is much smaller than the total cross-sectional area of the specimen as shown in Figure 9(a). Since the local fiber volume fraction in the fiber embedded area should be constant, as schematically shown in Figure 9(b); the number of carbon fibers was used as a parameter for discussing fracture modes.

The compressive failure of carbon fibers after the compression test is shown in Figure 10, which was taken when the compressive load was completely removed after fiber fracture. Fiber crush was observed when the number of carbon fibers was small as shown in Figure 10(a) to Figure 10(d). This is similar to compressive failure of a single-fiber model composite. Fractures propagated at an angle β , which was dependent of the number of aligned carbon fibers. The fracture angle β decreased slightly as the number of carbon fibers increased. By contrast, kink-band failure was observed when the number of carbon fiber was large as shown in Figure 10(e) to Figure 10(g). The kink-band angle (also expressed using β) decreased as the number of carbon fibers increased. The kink-band width w increased as the number of carbon fibers increased. Kink-band parameters, *i.e.*, kink-band angle and kink-band width were dependent on the number of adjacent carbon fibers.

The results are summarized in Figure 11. In the case of a unidirectional CFRP with approximately 60% fiber volume fraction, the kink-band angle was $5^\circ - 30^\circ$ and the kink-band width was 60 - 150 μm [3] [7] [11] [15] [17]. The kink-band parameters for the 11,000 fibers model composite were approaching that of the unidirectional CFRP. The number of carbon fibers was an influencing factor on compressive failure of a unidirectional CFRP when fibers were closely aligned within the mutually interacting distance.

4. Conclusions

The longitudinal compression tests of several fiber model composites were performed to study compressive failure of a unidirectional CFRP. The aligned carbon fibers were embedded in an epoxy matrix while maintaining the local fiber volume fraction constant, and the effect of the number of carbon fibers on kink-band failure was studied. The results obtained in this paper were summarized as follows:

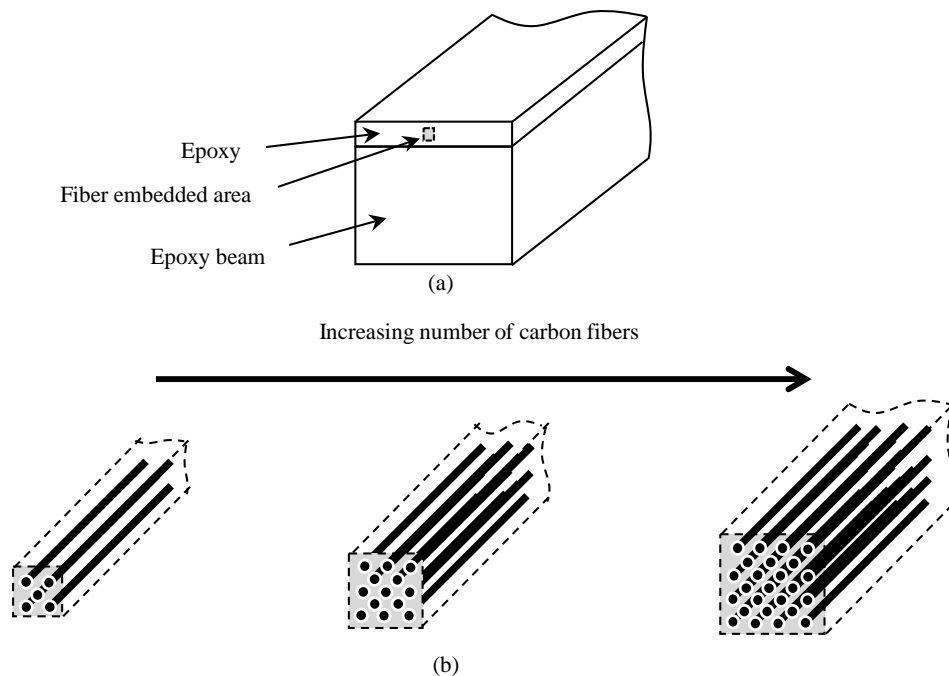


Figure 9. Fiber embedded area in multiple-fiber model composites. (a) Cross-section of a model composite; (b) Enlarged image of fiber embedded area (distance between each fiber is random but less than 15 μm).

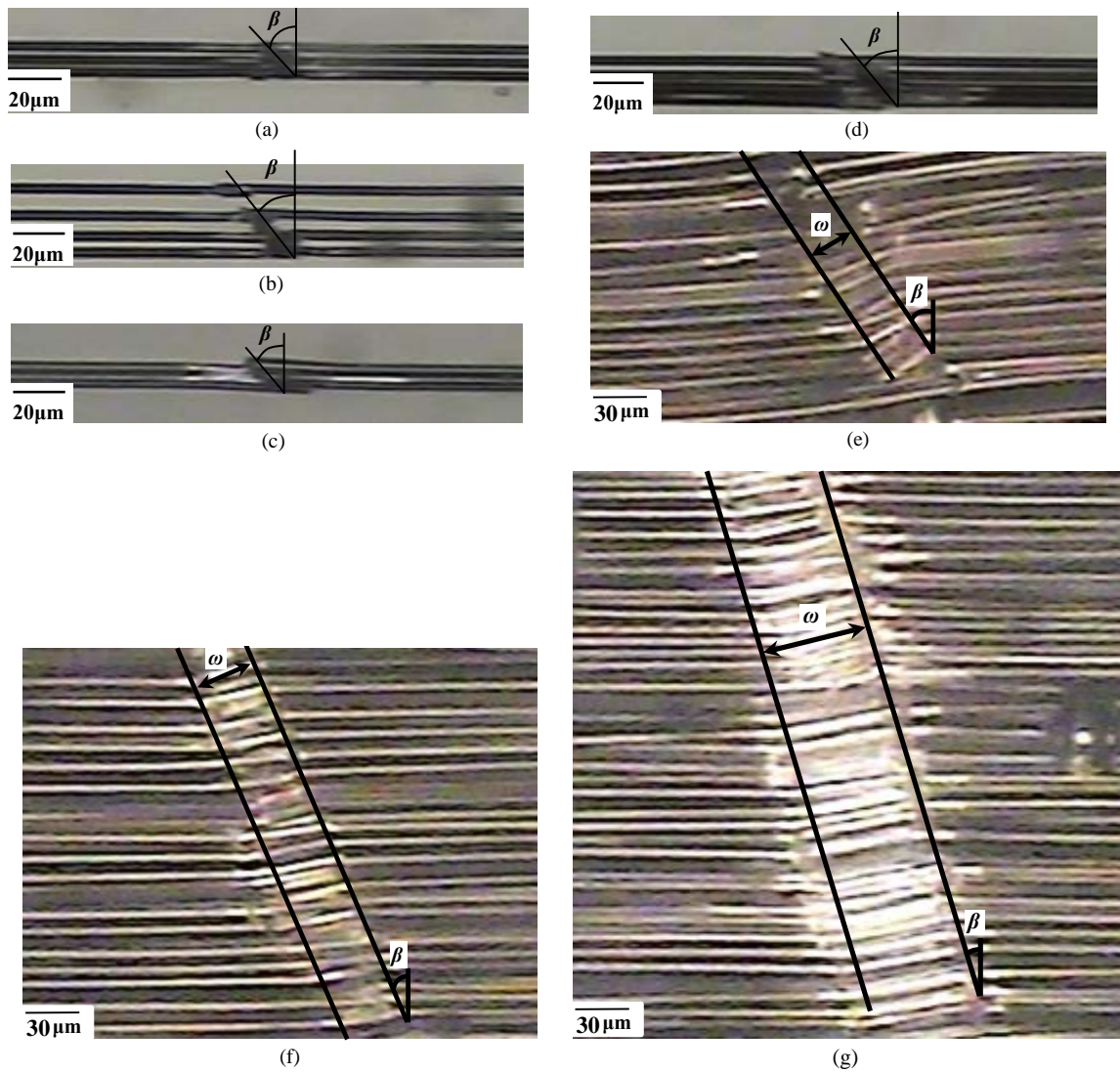


Figure 10. Compressive failure of multiple-fiber model composites. (a) Closely-aligned 3 fibers; (b) Closely-aligned 4 fibers; (c) Closely-aligned 8 fibers; (d) Closely-aligned 10 fibers; (e) Closely-aligned 530 fibers; (f) Closely-aligned 8000 fibers; (g) Closely-aligned 11,000 fibers.

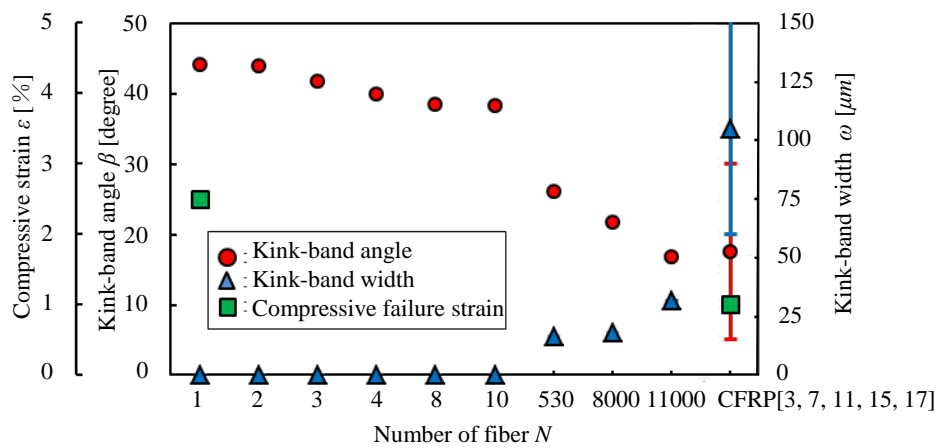


Figure 11. Kink-band angle, width and compressive strain versus number of fibers.

- 1) The single-fiber model composite failed by fiber crush. The fiber fractured in shear at an angle β . Compressive failure strain was much higher than that of a unidirectional CFRP.
- 2) The two-fiber model composites also failed by fiber crush. The two fibers failed at the same location which indicated mutual interaction of adjacent fibers during compressive failure when the distance between the fibers was small.
- 3) The fracture modes of the multiple-fiber model composites were dependent on the number of carbon fibers. When the number of carbon fibers was small, the failure mechanism was fiber crush. For a large number of carbon fibers, the failure mechanism was kink-band failure. Therefore, the longitudinal compressive failure mode shifted from fiber crush to kink-band as the number of carbon fibers increased. The kink-band parameters, *i.e.*, kink-band width and kink-band angle, were dependent on the number of closely-aligned carbon fibers, which could also affect resultant compressive strength.

References

- [1] Toray Technical Data Sheet, No. CFA-008(T1000G).
- [2] Ueda, M., Saito, W., Imahori, R., Kanazawa, D. and Jeong, T.K. (2014) Longitudinal Direct Compression Test of a Single Carbon Fiber in a Scanning Electron Microscope. *Composites Part A*, **67**, 96-101. <http://www.sciencedirect.com/science/article/pii/S1359835X14002541>
<http://dx.doi.org/10.1016/j.compositesa.2014.08.021>
- [3] Soutis, C., Curtis, P.T. and Fleck, N.A. (1993) Compressive Failure of Notched Carbon Fibre Composite. *Mathematical and Physical Sciences*, **440**, 241-256. http://www.jstor.org/stable/52233?seq=1#page_scan_tab_contents
- [4] Kyriakides, S., Arseculeratne, R., Perry, E.J. and Liechti, K.M. (1995) On the Compressive Failure of Fiber Reinforced Composites. *International Journal of Solids and Structures*, **32**, 689-738. <http://www.sciencedirect.com/science/article/pii/002076839400157R>
[http://dx.doi.org/10.1016/0020-7683\(94\)00157-R](http://dx.doi.org/10.1016/0020-7683(94)00157-R)
- [5] Morgan, P.M., Liu, X.U. and Shih, C.F. (1995) Kink Band Formation and Band Broadening in Fiber Composites under Compressive Loading. *Acta Metallurgica et Materialia*, **43**, 2943-2958. <http://www.sciencedirect.com/science/article/pii/095671519500001C>
[http://dx.doi.org/10.1016/0956-7151\(95\)00001-C](http://dx.doi.org/10.1016/0956-7151(95)00001-C)
- [6] Berbinau, P., Soutis, C. and Guz, I.A. (1999) Compressive Failure of 0° Unidirectional Carbon-Fibre-Reinforced Plastic (CFRP) Laminates by Fibre Microbuckling. *Composites Science and Technology*, **59**, 1451-1455. <http://www.sciencedirect.com/science/article/pii/S026635389800181X>
[http://dx.doi.org/10.1016/S0266-3538\(98\)00181-X](http://dx.doi.org/10.1016/S0266-3538(98)00181-X)
- [7] Soutis, C. and Curtis, P.T. (2000) A Method for Predicting the Fracture Toughness of CFRP Laminates Failing by Fibre Microbuckling. *Composites Part A*, **31**, 733-740. <http://www.sciencedirect.com/science/article/pii/S1359835X00000038>
[http://dx.doi.org/10.1016/S1359-835X\(00\)00003-8](http://dx.doi.org/10.1016/S1359-835X(00)00003-8)
- [8] Vogler, T.J. and Kyriakides, S. (2001) On the Initiation and Growth of Kink Bands in Fiber Composites: Part I. Experiments. *International Journal of Solids and Structures*, **38**, 2639-2651. <http://www.sciencedirect.com/science/article/pii/S0020768300001748>
- [9] Vogler, T.J., Hsu, S.Y. and Kyriakides, S. (2001) On the Initiation and Growth of Kink Bands in Fiber Composites. Part II: Analysis. *International Journal of Solids and Structures*, **38**, 2653-2682. <http://www.sciencedirect.com/science/article/pii/S002076830000175X>
- [10] Sutcliffe, M.P.F. and Yumono, A.H. (2001) Experimental Study of Microbuckle Initiation in a Model Composite System. *Scripta Materialia*, **45**, 831-837. <http://www.sciencedirect.com/science/article/pii/S1359646201011022>
[http://dx.doi.org/10.1016/s1359-6462\(01\)01102-2](http://dx.doi.org/10.1016/s1359-6462(01)01102-2)
- [11] Lee, J. and Soutis, C. (2007) A Study on the Compressive Strength of Thick Carbon Fibre—Epoxy Laminates. *Composites Science and Technology*, **67**, 2015-2026. <http://www.sciencedirect.com/science/article/pii/S0266353806004520>
- [12] Pimenta, S., Gutkin, R., Pinho, S.T. and Robinson, P. (2009) A Micromechanical Model for Kink-Band Formation: Part I—Experimental Study and Numerical Modelling. *Composites Science and Technology*, **69**, 948-955. <http://www.sciencedirect.com/science/article/pii/S026635380900061X>
- [13] Pimenta, S., Gutkin, R., Pinho, S.T. and Robinson, P. (2009) A Micromechanical Model for Kink-Band Formation: Part II—Analytical Modelling. *Composites Science and Technology*, **69**, 956-964. <http://www.sciencedirect.com/science/article/pii/S0266353809000529>
- [14] Jumahat, A., Soutis, C., Jones, F.R. and Hodzic, A. (2010) Fracture Mechanisms and Failure Analysis of Carbon Fi-

- bre/Toughened Epoxy Composites Subjected to Compressive Loading. *Composite Structures*, **92**, 295-305.
<http://www.sciencedirect.com/science/article/pii/S0263822309002839>
- [15] Gutkin, R., Pinho, S.T., Robinson, P. and Curtis, P.T. (2010) On the Transition from Shear-Driven Fibre Compressive Failure to Fibre Kinking in Notched CFRP Laminates under Longitudinal Compression. *Composites Science and Technology*, **70**, 1223-1231. <http://www.sciencedirect.com/science/article/pii/S0266353810001119>
- [16] Hapke, J., Gehrig, F., Huber, N., Schulte, K. and Lilleodden, E.T. (2011) Compressive Failure of UD-CFRP Containing Void Defects: *In Situ* SEM Microanalysis. *Composites Science and Technology*, **71**, 1242-1249.
<http://www.sciencedirect.com/science/article/pii/S0266353811001424>
- [17] Ueda, M., Mimura, K. and Jeong, T.K. (2014) *In Situ* Observation of Kink-Band Formation in a Unidirectional Carbon Fiber Reinforced Plastic by X-Ray Computed Tomography Imaging. *Advanced Composite Materials* (in Press).
- [18] Hawthorne, H.M. and Teghtsoonian, E. (1975) Axial Compression Fracture in Carbon Fibres. *Journal of Material Science*, **10**, 41-51. <http://link.springer.com/article/10.1007/BF00541030>
- [19] Deteresa, S.J. (1991) Piezoresistivity and Failure of Carbon Filaments in Axial Compression. *Carbon*, **29**, 397-409.
<http://www.sciencedirect.com/science/article/pii/0008622391902092>
- [20] Nishi, Y. and Hirano, M. (2007) Bending Stress Dependent Electrical Resistivity of Carbon Fiber in Polymer for Health Monitoring System. *Journal of Material Science*, **48**, 2735-2738.
<http://dx.doi.org/10.2320/matertrans.mra2007105>
- [21] Tanaka, F., Okabe, T., Okuda, H., Kinloch, I.A. and Young, R.A. (2013) The Effect of Nanostructure upon the Compressive Strength of Carbon Fibres. *Journal of Material Science*, **48**, 2104-2110.
<http://link.springer.com/article/10.1007/s10853-012-6984-z>
- [22] Liebig, W.V., Leopold, C. and Schulte, K. (2013) Photoelastic Study of Stresses in the Vicinity of a Unique Void in a Fibre-Reinforced Model Composite under Compression. *Composites Science and Technology*, **84**, 72-77.
<http://www.sciencedirect.com/science/article/pii/S026635381300167X>
- [23] Jeong, T.K., Ueda, M. and Hiraga, A. (2015) Measurement of a Longitudinal Compressive Modulus of Carbon Fiber Using a Single-Fiber Model Composite. *Material System*, **33**, 13-19. (In Japanese)
- [24] Liebig, W.V., Vies, C., Schulte, K. and Fiedler, B. (2015) Influence of Voids on the Compressive Failure Behaviour of Fibre-Reinforced Composites. *Composites Science and Technology*, **117**, 225-233.
<http://www.sciencedirect.com/science/article/pii/S0266353815300294>
- [25] Toray Technical Data Sheet, No. CFA-019(T800S).
- [26] ASTM Standard D695-02a (2002) Compressive Properties of Rigid Plastics. ASTM International.